

Research Article

Response of *Candidatus Liberibacter Asiaticus*-Infected Citrus Plants to *Bacillus amyloliquefaciens* GJ1

Tang JZ¹, Ding YX¹, Deng L¹, Nan J¹, Yang XY¹, Zhao XY² and JIANG L^{1*}

¹Key Laboratory of Horticultural Plant Biology of Ministry of Education, Huazhong Agricultural University, China

²State Key Laboratory of Agricultural Microbiology, Huazhong Agricultural University, China

*Corresponding author: JIANG L, Key Laboratory of Horticultural Plant Biology of Ministry of Education, Huazhong Agricultural University, National Indoor Conservation Center of Virus-free Germplasm of Fruit Crops, Wuhan 430070, China

Received: December 26, 2017; Accepted: March 16, 2018; Published: March 23, 2018

Abstract

Huanglongbing (HLB) is a major disease limiting citrus production worldwide. In this study, a new potential biocontrol agent *Bacillus amyloliquefaciens* GJ1 against HLB was employed to resistance disease experiment. We utilized isobaric tags for relative and absolute quantification-based quantitative proteomics approach for comparative analysis of protein abundances with *Candidatus Liberibacter asiaticus*-infected leaves treated and untreated by solution of *B. amyloliquefaciens* GJ1 ($OD_{600\text{ nm}} \approx 1$). The result revealed Differential Abundance Protein (DAP) of 21 expression-increased ($FC > 1.2$, $P\text{-value} < 0.05$) and 43 expression-decreased ($FC \leq 0.83$, $P\text{-value} < 0.05$) and COG classification annotation proteins were elucidated. Among them, the proteins involved in carbohydrate transport and metabolism were analyzed. *Bacillus amyloliquefaciens* GJ1 treatment brought about decreasing both of the content of the starch and the soluble sugar in leaves was proved, the function of starch degradation caused by *B. amyloliquefaciens* GJ1 treatment was proven via $I_2\text{-KI}$ test in roots. This study highlight one of the reasons in HLB biocontrol in citrus.

Keywords: Huanglongbing (HLB); *Bacillus amyloliquefaciens* GJ1; *Candidatus Liberibacter Asiaticus*; isobaric Tags for Relative and Absolute Quantification (iTRAQ); Degradation starch

Abbreviations

COG: Orthologous Groups of proteins; DAP: Differential Abundance Protein; GC: Gas Chromatography analysis; HLB: Huanglongbing; KEGG: Kyoto Encyclopedia of Genes and Genomes; qPCR: Real time quantitative PCR detecting system; iTRAQ: isobaric Tags for Relative and Absolute Quantification

Introduction

Citrus Huanglongbing (Huanglongbing, HLB) is considered to be one of the most devastating diseases threatening citrus production worldwide, and all cultivated citrus are susceptible to the disease in different degree. The pathogen mainly are vectored by the Asian psyllid [1], it is caused by three species of Gram-negative, α -proteobacteria, *Candidatus Liberibacter* spp. “*Ca. L.asiaticus*”, “*Ca. L.africanus*”, “*Ca. L.americus*” [2, 3 & 4]. The disease can also be transmitted to healthy trees by grafting of diseased bud wood [5]. Typical symptoms of Huanglongbing disease in leaves include shoot yellowing and blotchy mottled leaves, and in fruits express small, asymmetric, acidic, with many aborted seeds. The callose deposition occurs specifically in midribs of leaves [6]. Disordered cambial tissue and massive accumulation of starch in phloem have also been reported [6, 7 & 8]. HLB has led to the devastating harm of citrus in more than 40 countries [1,9]. HLB has not only decreased citrus production but also greatly increased production costs [10]. HLB has reached epidemic proportions in Florida and has caused more than \$4 billion in economic losses between 2005 to 2011.

A variety of ways have been adopted to control HLB over the past few decades, for instance, heavy pruning [11], inputting

antibiotic agents [12], inhibiting the *LdtR* gene by an inhibitor [13] and screening the combination of stock and scion [14]. However, the above mentioned techniques used for solving the problem of HLB present some limitations. Management of HLB to enable the continued economic production of citrus is the largest challenge ever faced by the citrus industry, and new control strategies are urgently needed.

Recent advances on host-pathogen interactions, genetics of different varieties, and resistance mechanism are discussed in HLB [15]. Reported that Pathogen-Associated Molecular Patterns (PAMP) activity of *flg22* in *Las* is weaker than those in other well-studied plant pathogenic bacteria [16]. Predecessors thought that host citrus plants have not evolved sufficient immune responses to effectively prevent infection [17]. Given the availability of high-throughput sequencing, transcriptomes and proteomes have been applied to *Las*-infected plants and treated plants; as a result, numerous characteristic innate immunity elicitors, transcription factors, defense responsive components, and signaling molecules have been discovered [18 - 22]. However, the resistance metabolism of HLB remains unknown. *Bacillus* sp. Is a biological control agent that can control diseases to a host animal or plant, thereby preventing the development of disease by a pathogen [23]. *Bacillus* sp. is widely distributed in nature and harmless to humans and animals. *Bacillus* belongs mostly to endogenous spores, reproduces rapidly, and can be easily colonized on the surface of plant roots. It can produce a series of metabolites during growth. The antibacterial substances of *Bacillus* include antimicrobial protein, lipid peptide and polyketone, secretory proteins, enzymes etc. [24] The different genes involved in the metabolite synthesis in *B. amyloliquefaciens* FZB42 were

determined. *Bacillus bacillus* is the dominant microbial population in soil and nature. Biological control agents have developed numerous success stories in the field of plant disease resistance. Previous studies have shown that *B. amyloliquefaciens* FZB42 is a highly successful example for plant disease resistance [25, 26]. The above mentioned reports have proven that *B. amyloliquefaciens* is a powerful biocontrol agent against plant diseases.

Carbohydrate transport and metabolism are closely related to the infection and control of HLB disease. Sucrose phosphate synthase is an important control point in the synthesis of sucrose [27]. The enzymes of sucrose degradation are sucrose invertase and sucrose synthase. The direct precursor of starch synthesis is adenosine diphosphate glucose. Starch is formed via ADP-glucose pyrophosphorylase, which catalyzes the reaction between glucose-1-phosphate and ATP. Amylose synthase is directly related to starch content and the ratio of amylose and amylopectin [28]. The degradation of starch in leaves involves three pathways: maltose pathway, glucose pathway, and G-1-P pathway. The phosphorylation of starch granules in leaves influences the hydrophilicity of starch granules, thereby affecting starch degradation [29]. The enzymes related mainly to phosphorylation are glucan water dikinase and phosphate glucan hydration kinase. During starch degradation, α -amylase and β -amylase play key roles. The expression levels of many proteins involved in carbohydrate metabolism are affected by Las infection. Proteins that participate in starch synthesis and starch granules synthesis are unregulated by Las infection [6, 7 & 22].

In this study, we attempted to investigate the responses of Las-infected host citrus plants to a newly screened *B. amyloliquefaciens* GJ1 with the aid of iTRAQ-based proteomics analysis. In particular, the annotation proteins related to “carbohydrate transport and metabolism” were concerned. We also detected several physiological indices of soluble sugar, starch, fructose, sucrose and glucose, and the I_2 -KI reaction, in order to clarify the affect on the carbohydrates, while the infected plants treated by *B. amyloliquefaciens* GJ1. Understanding of the mechanisms is crucial for the isolation of effective biocontrol agents and the further development of biocontrol strategies for HLB.

Materials and Methods

Preparation of plant material

The infected plants by *Ca. L. asiaticus*-infected (Las) and health plants of *Citrus madurensis* Lour were used for measurement of the physiological index, all the plants were grown under the same soil condition and management. Las-infected plants treated and untreated (CK) by *B. amyloliquefaciens* GJ1 were carried out in *Citrus sinensis* (L.) Osbeck grown in a greenhouse. HLB was detected with QPCR and PCR in advance, and the Las positive plants were used for subsequent tests. Both treated and control plants were grown in the same soil condition in a plastic pot, the normal soil irrigated the supplementary 1/8 MS mineral element 0.5 L/plant and 200 mg/L polypeptide (patent number: CN1827560A) once a month. Above mentioned the supplementary solution can be called “A solution”. *Bacillus* was applied *via* root irrigation once every 7 days. Each plant was irrigated with 1.5 L of treatment bacteria solution.

Protein preparation and iTRAQ labeling

The leaves were milled to powder in mortar with liquid nitrogen.

Subsequently, 150 mg of powder from each sample was mixed with 1 mL of lyses buffer containing Tris-base pH=8, 7M Urea, 2 M Thiourea, 0.1% SDS, 2 mM EDTA, Protease inhibitor cocktail (Roche), 1 mM phenyl methyl sulfonyl fluoride in a glass homogenizer. Homogenates were incubated on the ice for 20 min and then centrifuged at 12000 g for 15 min at 4°C; the supernatant was transferred to a new tube. Protein concentrations were determined by Bradford assay.

The supernatant containing precisely 100 μ g protein of each sample was digested with Trypsin (Promega, Madison) at 37°C for 16 h. After trypsin digestion, peptides were dried by vacuum centrifugation. Desalted peptides were labeled with iTRAQ reagents (iTRAQ® Reagent-8PLEX Multiplex Kit, 4381663) according to the manufacturer's instructions (AB Scitex, Foster City, CA). For 100 μ g peptide 1 units of labeling reagent were used. Peptides were dissolved in 20 μ l of 0.5 M TEAB (Triethylammonium Bicarbonate) pH 8.5 solution and labeling reagent was added in 70 μ l of isopropanol. After 1h incubation the reaction was stopped with 50 mM Tris-HCl pH 7.5. The labeled peptides were incubated for 2h at room temperature. Differentially labeled peptides were mixed.

HPLC fractionation and LC-MS/MS analysis

RP separation in the first dimension by micro LC was performed on an L-3000 HPLC System (Rigol) using a Dura shell RP column. Mobile phases A (2% acetonitrile, 20 mM NH_4FA , pH was adjusted to 10.0 using $\text{NH}_3\cdot\text{H}_2\text{O}$) and B (98% acetonitrile, 20 mM NH_4FA , pH was adjusted to 10.0 using $\text{NH}_3\cdot\text{H}_2\text{O}$) were used to develop a gradient elution. Fractions from the first RPLC dimension were dissolved with loading buffer and then separated by a C18 column (75 μ m inner diameters, 360 μ m outer diameter \times 10 cm, 3 μ m C18). Mobile phase A consisted of 0.1% formic acid in water solution, where as mobile phase B consisted of 0.1% formic acid in acetonitrile solution. A series of adjusted linear gradients was applied based on the hydrophobicity of fractions eluted in 1D LC with a flow rate of 300 nL/min. For Orbitrap Q Exactive, the source was operated at 1.8 kV. For full MS survey scan, the AGC target was $3e6$ and the scan range was from 350 to 1800 with a resolution of 70,000. The 20 most intense peaks with charge state 2 and above were selected for fragmentation by HCD with normalized collision energy of 32% for iTRAQ-labeled peptides. The MS2 spectra were acquired with 17, 500 resolution.

Data analysis of proteins

The MS raw data files from Q-Exactive were first searched by Mascot (Matrix Science, London, UK; version 2.6.0). Mascot was set up to search the Swiss rot database assuming the digestion enzyme trypsin. Mascot was searched with a fragment ion mass tolerance of 0.020 Da and a parent ion tolerance of 10.0 PPM. Carbamidomethyl of cysteine and iTRAQ8plex of lysine and the n-terminus were specified in Mascot as fixed modifications. Oxidation of methionine, acetyl of the n-terminus and iTRAQ8plex of tyrosine were specified in Mascot as variable modifications. Protein identifications were accepted if they could be established at greater than 90.0% probability to achieve an FDR less than 10.0% and contained at least 2 identified peptides. We only used ratios with p -values \leq 0.05, and only ratio of >1.2 were considered as significant. We used databases, namely, Clusters of Orthologous Groups (<http://www.ncbi.nlm.nih.gov/COG/>), and (<http://citrus.hzau.edu.cn/orange/download/csi.peptide.fa.tar.gz>) to predict gene functions.

Determination of soluble sugar by anthrone colorimetry

Anthrone colorimetry was conducted following previously reported instructions [30]. Anthrone reagent and stock standard were prepared, and the working standard was obtained. A blank solution was simultaneously prepared, and a calibration curve was constructed. The sugar concentration in the samples was computed from the calibration curve. Samples were collected for five biological repeats. Statistical analyses of differences among groups were determined using the t-test. The correlation index R^2 was 0.9959.

Determination of total starch content via iodization method

The total starch content was determined via iodization method [30]. The standard curve and iodine were prepared. Soluble starch was extracted, and color measurement was performed. In brief, 2 mL of sample extract was drawn in a calibration tube and added with 0.1 mL of I_2 -KI solution. The following steps were the same as those in the determination of the standard curve. Finally, absorbance values of samples were measured, and the total starch content was calculated. Samples were collected for three biological repeats. Statistical analyses were performed using the t-test. The correlation index $R^2=0.9988$ of the standard curve.

Determination of amylose and amylopectin via the dual wavelength method

The dual wavelength method was conducted to analyze the amylose and amylopectin contents severally [31]. Standard liquid and starch scanning liquid were prepared. Amylose standard and amylopectin standard curves were constructed, and samples were then prepared. Approximately 0.1000 g of samples was mixed with 10 mL of 0.5 M KOH, stirred in a 60°C water bath, heated for 10 min, transferred to a 50 mL flask, and added with distilled water to reach a constant volume. Subsequently, 2.5 mL of the sample mixture, to a 50 mL flask, added 30 distilled water and adjusted pH with hydrochloric acid solution to 3.5, added 0.5 mL of iodine solution and filled to scale with distilled water. After 30 min, the solution was shaken well. And the starch scanning fluid was scanned by a spectrophotometer. The measurement wavelength of amylose was 603 nm, and the reference wavelength of amylose was 450 nm. By contrast, the measurement wavelength of amylopectin was 526 nm, and the reference wavelength of amylopectin was 730 nm. Samples were collected for three biological repeats. Statistical analyses were conducted using t-test. In the study, the correlation exponent of the standard curve of amylose was $R^2=0.9938$, where as the correlation index of the standard curve of amylopectin was $R^2=0.9968$.

Determination of fructose, sucrose, and glucose contents by gas chromatography analysis (GC)

We prepared a single sample and mixed samples of fructose, sucrose, and glucose severally. Derivatization and preparation of samples was performed, dry material was crushed, blended, weighed the sample of 0.05 g and placed in a test tube, added with 7 mL of distilled water, and sealed with plastic film. After boiling water bath extraction for 30 min, the filtrate was extracted and transferred to a 10 mL volumetric flask. Take 200 μ l internal standard and add the distilled water to a calibration tube. Shake well, place for 1 hour, and take 1 ml solution into 1.5 ml centrifuge tube, and perform centrifugation 20 mins (10000 g) (repeat one time). GC analysis was

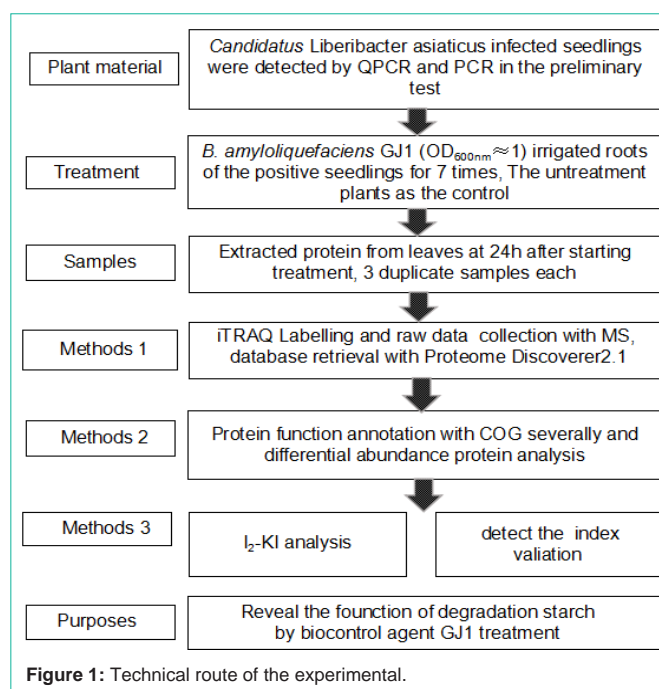


Figure 1: Technical route of the experimental.

conducted using a chromatographic column under the following conditions: HP-5 capillary column (5%-phenyl-methyl polysiloxane, 30 m \times 25 μ m i.d. \times 0.1 μ m); injection port temperature, 270°C; test temperature, 300°C; high purity nitrogen as carrier gas, flow rate 25 mL/min; hydrogen, flow rate 30 mL/min; air, flow rate 400 mL/min; cylinder head pressure, 12.00 psi; sample, 1 μ L; and shunt ratio, 60:1 [32]. Gas chromatography analysis with Agilent 6890N gas chromatograph (USA). The samples were collected for three biological repeats. Statistical analyses were conducted using the t-test.

Characteristic observation of root and leaves with I_2 -KI and measure of photosynthetic rate

Collect the fresh roots and leaves from plants of treated and untreated by GJ1, at least 4 biology repetitions. The roots were washed clear and staining with I_2 -KI for 30 mins. The veins via a hand slice and staining with I_2 -KI for 30 mins, and then observed with Olympus SZX16 Microscope (Japan). The photosynthetic rate was detected with Li-6400XT Portable Photosynthesis system. The technical route is shown below (Figure 1).

Results

Identification of differentially abundance proteins by iTRAQ

The total number of two level mass spectrometry was 34,031 which were generated from the iTRAQ experiment using Las-infected plants treated and untreated by *B. amyloliquefaciens* GJ1 as the materials. The number of identified segments was 11,343 and the number of identified proteins was 2106 (FDR<1%). Protein species were considered differentially accumulated when they exhibited an up regulation with fold change >1.2 and $p<0.05$ and a down regulation with fold change ≤ 0.83 , $p<0.05$, and FDR <1%. Under these two criteria, Differential Abundance Protein (DAP) species were identified in Las-infected plants treated and untreated by *B. amyloliquefaciens* GJ1 potted seedlings. Significantly up regulated

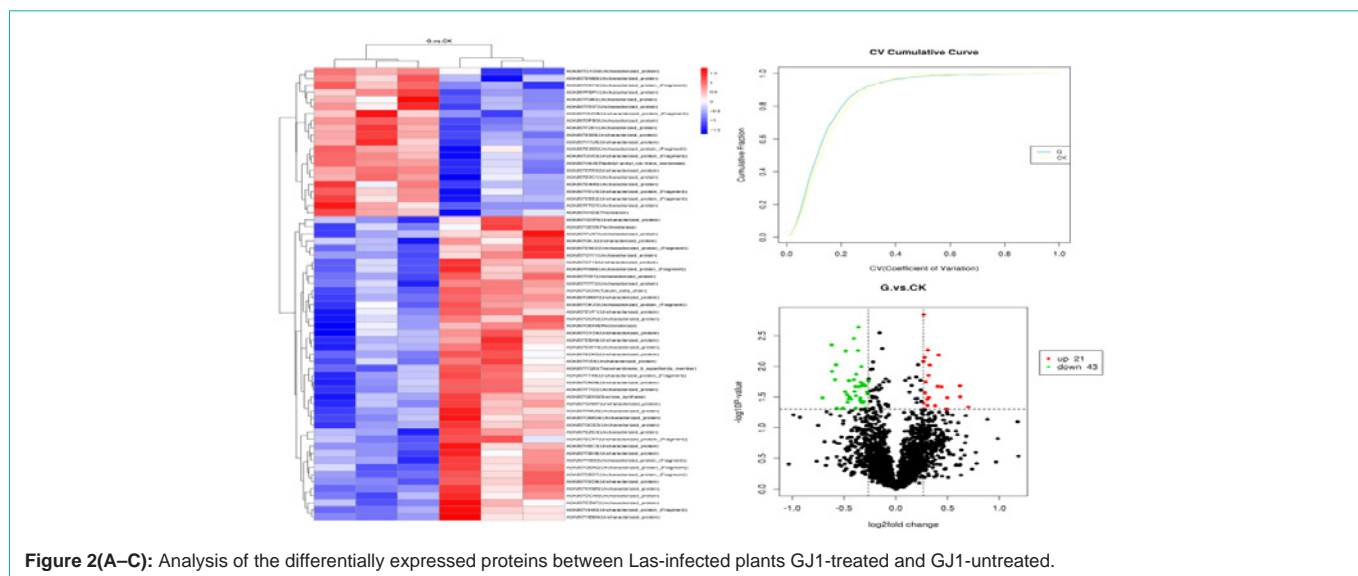


Figure 2(A–C): Analysis of the differentially expressed proteins between Las-infected plants GJ1-treated and GJ1-untreated.

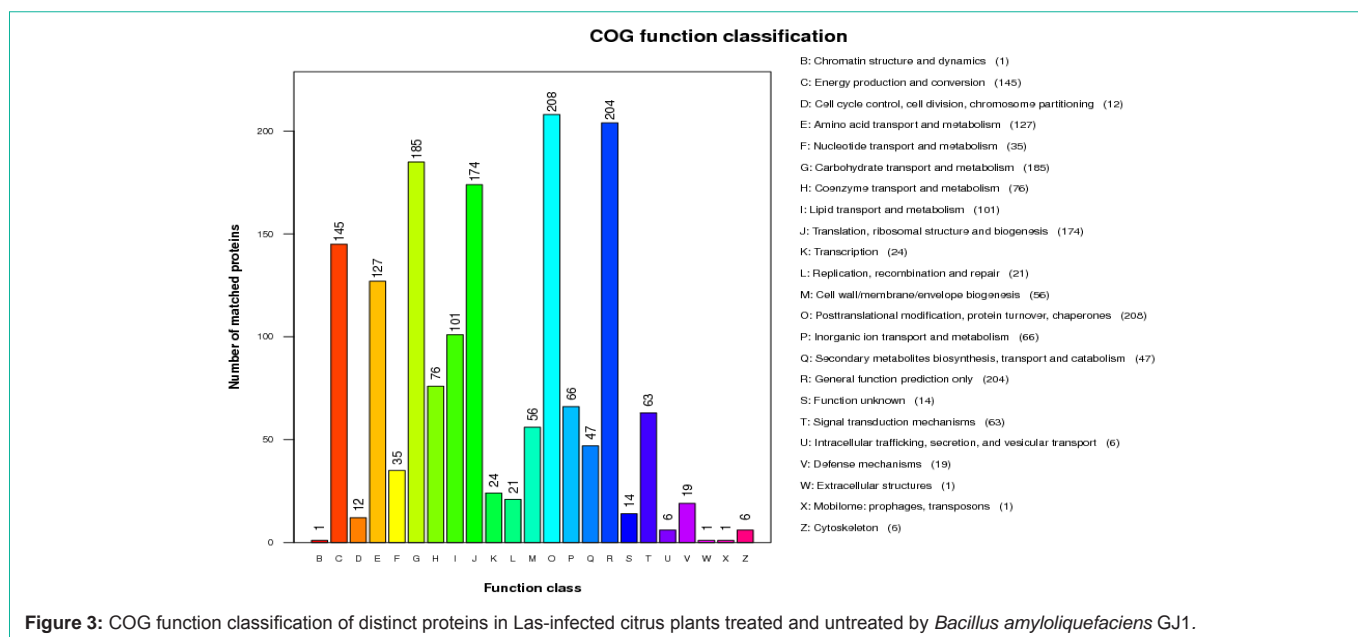


Figure 3: COG function classification of distinct proteins in Las-infected citrus plants treated and untreated by *Bacillus amyloliquefaciens* GJ1.

proteins were labeled red in GJ1-treated samples and labeled blue in GJ1-untreated samples. By contrast, significantly down regulated proteins were labeled blue in GJ1-treated samples and labeled red in GJ1-untreated samples. A total of 64 DAPS were identified, of which 21 were increased-accumulated and shared 32.8% of the identified DAP proteins, and 43 were decreased-accumulated and shared 67.2% of the identified DAP proteins in the heat map (Figure 2A) and volcano plot (Figure 2B). Detailed information is provided in (Supplementary Table 1). The cumulative graph of all the protein Coefficients of Variance (CVs) in the corresponding samples showed that the faster the curve raised, the better the overall repeatability of the samples (Figure 2C).

Figure 2(A-C) analysis of the differentially expressed proteins between Las-infected plants GJ1-treated and GJ1-untreated. A. Hierarchical cluster analysis of GJ1-responsive differentially

expression proteins. The vertical is the clustering of samples (three repetitions). B. Volcano plot of differentially expressed proteins. X-axis represents proteins expressing two changes in different samples. Y-axis represents the statistically significant differences of protein expression quantity changes (pad $j < 0.05$). Red dots indicate significant up regulation in differentially expressed proteins, whereas green point shows significant down regulation in differentially expressed proteins. C. Coefficient of Variance (CV) analysis of repeatability.

COG annotation of the protein species in *B. amyloliquefaciens* GJ1 treatment

Each COG consists of individual orthologous proteins. Orthologs typically have the same function, allowing transfer of functional information from one member to an entire COG. In this experiment, the COGs comprised a framework for functions related to Las-

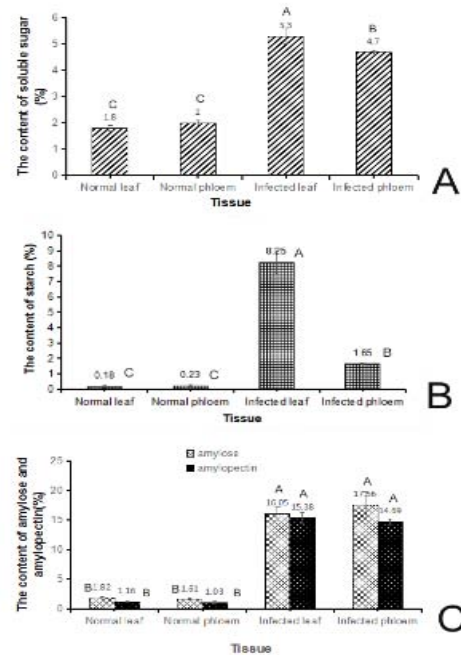


Figure 4(A-C): Comparison of four indices in healthy citrus and Las-affected citrus. (A) Soluble sugar. (B) Starch. (C) Amylose and amylopectin

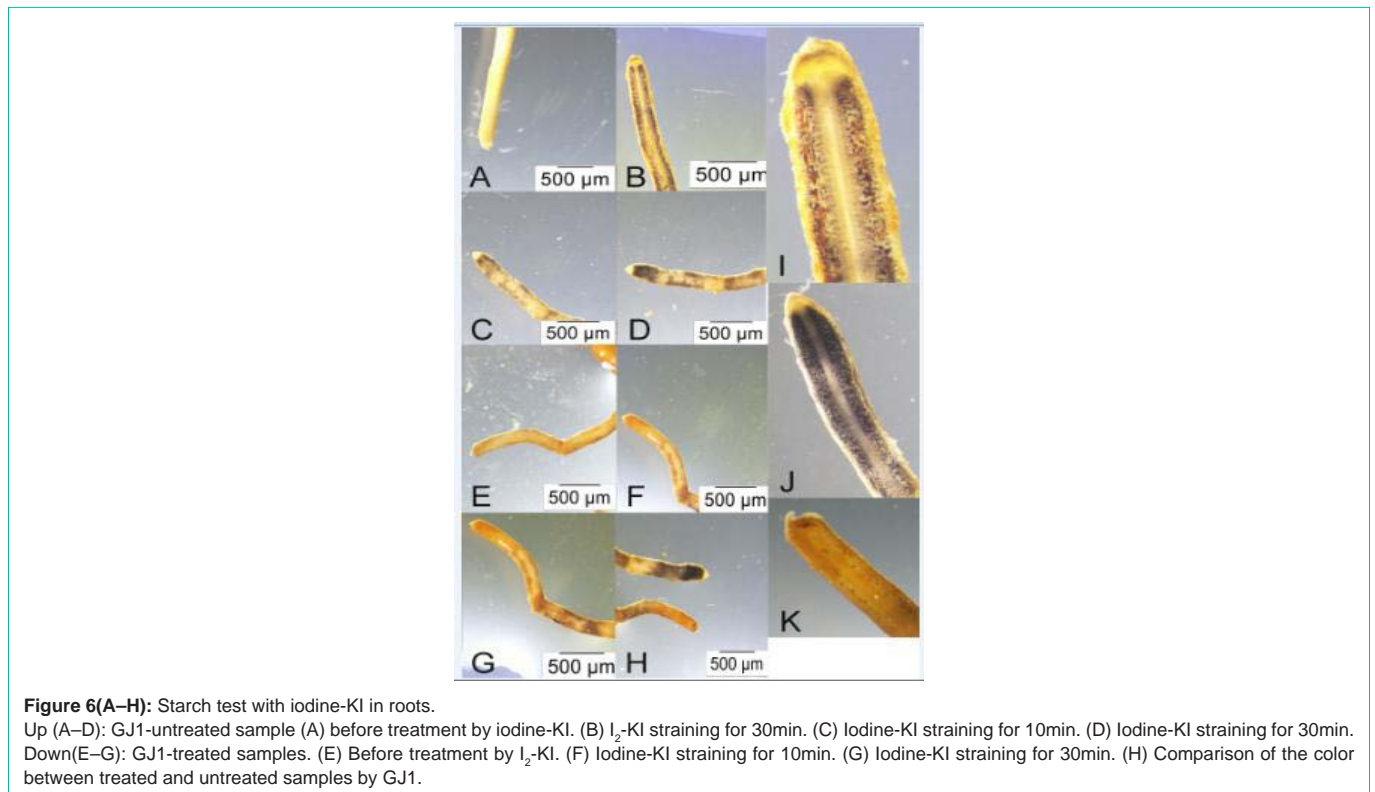
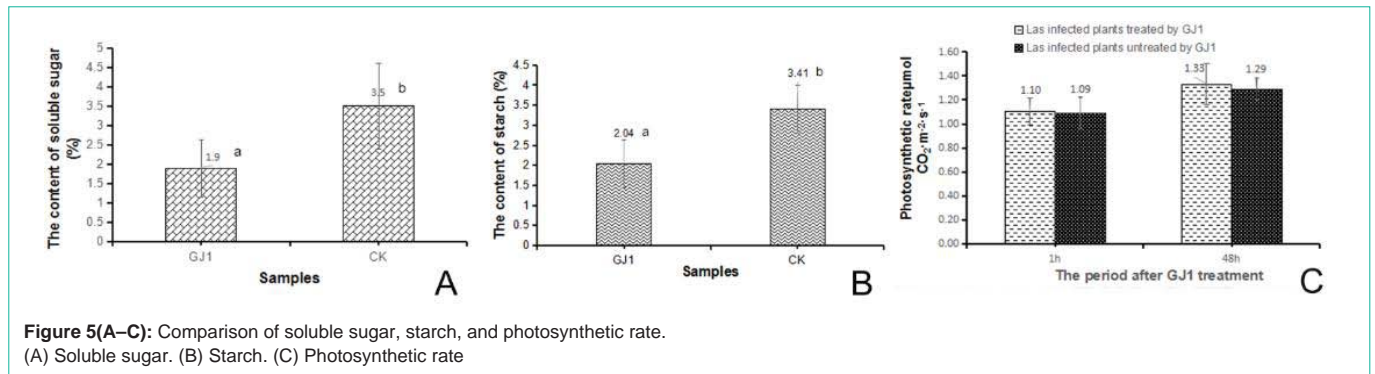
infected citrus plants treated and untreated by *B. amyloliquefaciens* GJ1. Twenty-three functional classes were produced by COG. The abbreviations and interpret in (Figure 3) are as follows: B, chromatin structure and dynamics; C, energy production and conversion; D, cell cycle control, cell division, and chromosome partitioning; E, amino acid transport and metabolism; F, nucleotide transport and metabolism; G, carbohydrate transport and metabolism; H, coenzyme transport and metabolism; I, lipid transport and metabolism; J, translation, ribosomal structure, and biogenesis; K, transcription; L, replication, recombination, and repair; M, cell wall/membrane/envelope biogenesis; O, posttranslational modification, protein turnover, and chaperones; P, inorganic ion transport and metabolism; Q, secondary metabolite biosynthesis, transport, and catabolism; R, general function prediction only; T, signal transduction mechanisms; U, Intracellular trafficking, secretion, and vesicular transport; V, defense mechanisms; W, extracellular structures; X, Mobilome: prophages and transposons; and Z, cytoskeleton. A total of 1592 proteins were annotated in COG (Figure 3). The protein number of each COG is shown in Figure 3. The group of “posttranslational modification, protein turnover, and chaperones” contained the most proteins (13% of the COG proteins). The function of the aforementioned 23 COG protein groups were stimulated by biological control agent’s *B. amyloliquefaciens* GJ1. Thus, multiple clues are provided to control HLB disease.

Characteristics of COG classification annotation proteins relate to “carbohydrate transport and metabolism”

The “carbohydrate transport and metabolism” in COG annotation protein group includes 185 proteins and shares 11.6% of COG annotation proteins. Among them, 59 proteins of known function are listed in (supplementary Table 2). Changes in the protein expression between the treatment and control groups were compared. The

expression levels of 22 proteins increased.

Ribulose-1,5-bisphosphate carboxylase/oxygenase (RuBPCO) large subunit (B7S512) was methyltransferase and transferase. Its protein expression increased by 51% compared with the control. The protein expression of starch synthase (A0A067EGP7), which belongs to the family of hexosyltransferases, specifically the glycosyltransferases, increased by 31.7% compared with the control. Biocontrol agent treatment promoted the demand for starch synthase in citrus plants after treatment with GJ1. Fructose-bisphosphate aldolase (A0A067DF17) is one of the important glycolytic isozymes in the metabolic process. Glyceraldehyde 3-Phosphate Dehydrogenase (GAPDH; A0A067GZQ5) can catalyzes the sixth step of glycolysis and serves to break down glucose for energy and carbon molecules. Pyruvate kinase (A0A067ETG2) is the enzyme that catalyzes the final step of glycolysis. It catalyzes the transfer of a phosphate group from Phosphoenolpyruvate (PEP) to Adenosine Diphosphate (ADP), yielding one molecule of pyruvate and one molecule of ATP. Phosphoglycerate kinase (PGK1; A0A067F2H8) is a transferase. PGK is a major enzyme used in glycolysis. In the first ATP-generating step of the glycolytic pathway, the expression levels of the four abovementioned proteins increased by 29.7%, 13.7%, 12.8%, and 9.7% as demonstrated by ITRAQ. β -Galactosidase (A0A067EQT1) is a glycoside hydrolase enzyme that catalyzes the hydrolysis of β -galactosides into monosaccharides. 6-Phosphogluconate dehydrogenase (6PGD; A0A067G3F9) is an enzyme in the pentose phosphate pathway. It forms ribulose 5-phosphate from 6-phosphogluconate. It is an oxidative carboxylase. Pectin lyase (A0A097PQV8), also known as pectolyase, is a naturally occurring pectinase that degrades pectin. Alpha-galactosidase (A0A067EQ43) is a glycoside hydrolase enzyme that hydrolyzes the terminal alpha-galactosyl moieties from glycolipids and glycoproteins. Beta-amylase



(A0A067F9K7) is an enzyme that acts on starch, glycogen, and related polysaccharides and oligosaccharides to produce beta-maltose *via* inversion. The expression levels of the five abovementioned proteins increased by 2.2%, 3.5%, 6.3%, 1%, and 1% severally, compared with untreated plants by GJ1. In addition, the expression levels of 34 proteins decreased, whereas three proteins showed almost no change (Supplementary Table 1). Specifically, we conjectures that starch synthase is normally needed when carbon metabolism trend to balanced.

Comparison of four physiological indexes between the Las-infected plants and healthy plants

Soluble sugar content: Test results display that the soluble sugar content in leaves and phloem was significantly higher than that in healthy leaves and healthy phloem. The soluble sugar content (5.3%) of the infected leaves was three times that of healthy leaves (1.8%). Therefore, HLB infection could increase the soluble sugar content in

the leaves and phloem of citrus (Figure 4A). All plants in this test didn't treated by GJ1.

Starch content: The total starch content in leaf and phloem varied significantly ($p < 0.01$) higher than that in healthy leaves and healthy phloem. The total starch content (8.25 mg/g) of the infected leaves was 46 times that in healthy leaves (0.18 mg/g). Therefore, the starch content in citrus leaves and phloem significantly increased after citrus infection (Figure 4B). All plants in this test didn't treated by GJ1.

The contents of amylose and amylopectin in healthy leaves and healthy phloem represented a consistent trend in the histogram. The starch content in the infected tissue was significantly ($p < 0.01$) higher than that in healthy tissues. For example, the amylose content in diseased leaves (15.38%) was 13 times higher than that in healthy leaves (1.16%), whereas the amylopectin content in diseased leaves (16.05%) was 8.81 times higher than that in healthy leaves (1.82%). These results were consistent with findings of the iodine staining

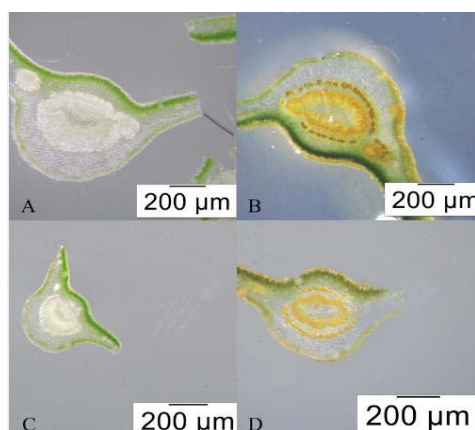


Figure 7(A–D): Starch test with iodine-KI in leaves.

A and B: Las-infected plant GJ1-untreated samples. C and D: Las-infected plant GJ1-treated samples.

Table 1: Comparing of three physiological indexes in health and Las-affected trees with GC.

Tissue	Fructose (mg/g)	Glucose (mg/g)	Sucrose (mg/g)
Healthy leaf	77.77±0.11C	85.42±0.20C	0.00±0.00D
Healthy phloem	80.48±1.03B	87.31±1.28C	7.27±4.14C
Infected leaf	89.41±0.71A	94.85±0.62A	28.58±2.81B
Infected phloem	81.53±0.64B	89.73±0.47B	64.23±1.68A

method. All plants in this test didn't treated by GJ1. When citrus was infected with HLB, starch accumulated in the citrus leaves and phloem (Figure 4C).

Gas Chromatography (GC) analysis of the differences in fructose, glucose, and sucrose

The contents of three kinds of sugar in these four tissues were determined by GC. When HLB was infected, the fructose content in citrus leaves varied significantly ($p < 0.01$). No significant change in the fructose content was found in citrus phloem. However, the glucose content increased significantly ($p < 0.01$) after infection with HLB, especially in the infected leaves, which showed higher glucose content than the phloem. The sucrose content increased significantly in citrus tissues after infection with HLB, which was consistent with previous soluble sugar results. Notably, the sucrose content was not detected in healthy leaves. After infection with HLB, the sucrose content both in leaves and phloem increased sharply, and that in phloem was always higher than that in the leaf (Table 1). All plants in this test didn't treated by GJ1.

Comparison of three indices with Las-infected plants treated and untreated by GJ1

All the positive plants were determined in advance. The data showed that the soluble sugar content in leaves of Las-infected plants untreated by GJ1 was significantly ($p < 0.05$) higher than that treated with GJ1 biocontrol agent. The soluble sugar content (3.5%) of the Las-infected GJ1 untreated leaves was 1.84 times that of GJ1-treated leaves (1.8%). The starch content demonstrated a similar trend to soluble sugar. The starch content in the leaves of untreated plants (3.4%) was slightly higher ($P < 0.05$) than that in GJ1-treated leaves (2.04%). Therefore, treatment with GJ1 could decrease the contents of

soluble sugar and starch compared with GJ1-untreated leaves (Figure 5A, 5B).

Under air temperature at 12°C, after Las-infected plants with GJ1-treatment for 1 and 48 h separately, the photosynthesis rate increased slightly by 3.1% in the GJ1-treated samples compared with that in GJ1-untreated samples (Figure 5C). However, the difference was not significant, further test at different temperature conditions are needed.

Characteristic observation of root and leaves with iodine staining

Root response: Usually, in the starch determination test, the direct addition of iodine-KI reagent on a material with starch will show a blue-black color, if starch is present. The amylose and iodine solution forms dark blue complex, and the amylopectin and iodide reaction is characterized by deep red or red. In this study, we found that the top of the roots was orange or yellow color on the surface when stained with iodine-KI reagent (Figure 6F& 6G), and the longitudinal section did not show any blue color in the Las-infected plants GJ1-treated by (Figure 6K). However, the surface of roots showed partly dark blue color and the time was longer with straining color deeper (Figure 6B, 6C and 6D), the longitudinal section of the roots showed dark blue and deep red granule in the GJ1-untreated plants (Figure 6I, 6J). Above results proved that *Bacillus Amyloliquefaciens* GJ1 produced the visible effect of degradation of amylase (Figure 6I, 6J and 6K). The samples (Figure 6A, 6E) showed normal before stained with iodine-KI reagent; both samples showed in the same picture stained for 30mins (Figure 6H). However, the quantitative analysis of starch needs to be improved further.

Response of leaves to iodine-KI: We investigated and found that the cross section of the veins remained orange or yellow and did not produce a blue color with iodine-KI staining in the Las-infected plants by GJ1-treated (Figure 7D), the cross section of the veins showed a slightly deep brown color in phloem with iodine-KI staining in Las-infected plants GJ1-untreated (Figure 7B). There was no blue color complex produced in both samples (Figure 7A - 7D). Whether *Bacillus Amyloliquefaciens* GJ1 cause the change of callosity and the PP₂ protein in phloem require further test verification.

Discussion

HLB seriously damages citrus production. The exploration of effective controlling techniques against HLB has become an important task at home and abroad. In our experiment, a new useful *B. amyloliquefaciens* GJ1 resistant HLB used for this study, and some of the detoxification responses were discovered with the aid of ITRAQ proteome label, the results revealed Differential Abundance Protein (DAP) of 21 expression-increased ($FC > 1.2$, $P\text{-value} < 0.05$) and 43 expression-decreased ($FC \leq 0.83$, $P\text{-value} < 0.05$) in Las-infected plants by GJ1-treated and untreated; and COG classification annotation proteins were elucidated; The functions of enzyme in “carbohydrate transport and metabolism” were analyzed; *B. Amyloliquefaciens* GJ1 treatment brought about the content decreasing of starch and soluble sugar and new visible evidence was found on degradation amylase in roots partly in Las-infected plants with GJ1-treated.

Prophase work basis of *B. amyloliquefaciens* GJ1

In our laboratory, a new strain of *B. amyloliquefaciens* GJ1 was selected and the patent application number has been obtained. We obtained a good detoxification rate in Las-infected plants after irrigation with $OD_{600nm} \approx 1$ *Bacillus* GJ1 solution for seven times. *B. amyloliquefaciens* GJ1 was registered in China Center for Type Culture Collection. In this experiment method, a polypeptide was added to both *B. amyloliquefaciens* GJ1 treatment and the control, and it might have contributed to HLB resistance *via* synergy or interaction of polypeptide and GJ1, the real cause of Huang long disease could be controlled needs to be discussed further.

Basic on the functions of GJ1, highlight the new strategy of resist Huang long disease

The starch content in leaves of Las-affected branches increased quickly compared with those from non-HLB trees. Starch not only over accumulates in photosynthetic cells, but starch grains become prominent in vascular parenchyma and sieve elements [33]. Sucrose accumulation in “*Ca. L. asiaticus*” - infected leaves suggests that photo assimilate translocation is impaired by “*Ca. L. asiaticus*” infection [25, 6 & 34]. These findings were in agreement with the present study. Observations about the contents of soluble sugar and starch in Las-infected and healthy citrus leaves and phloem revealed consistent results with previous studies. Interestingly, this test highlight that treatment of the biocontrol agent GJ1 decreased the soluble sugar and starch content compared with the Las-infected untreated plants by GJ1. It is important to inspire us to put forward the new strategy resist Huang long disease.

GJ1 treatment regulated the expression of enzymes in carbon metabolism

Huanglongbing disease interfered seriously the carbohydrate metabolism balance of citrus plants, according to the content change of soluble sugar, starch, fructose, sucrose and glucose in many reports [26, 27, 6, 21]. In this study, the treatment of *Bacillus Amyloliquefaciens* GJ1 could eliminate efficiently the pathogen of *Candidatus Liberibacter asiaticus*, it was speculated that one of the important reasons was that the enzyme related to carbohydrate transport and metabolism adjusted the balance of the carbohydrate metabolism.

Multiple data of up regulation of carbohydrate synthesis elements

and down regulation of photosynthesis components were observed in Las-infected citrus. The down regulation of genes encoding beta-amylase was involved in the degradation process [35, 6, 7, 22]. The accumulation of carbohydrate and starch could cause an inhibition of photosynthesis *via* a negative feedback mechanism [9]. *Ca. Asiaticus* lacks a glucose phosphotransferase system. Glucose is imported into the cell *via* a glucose/galactose transporter, which is present in *Ca. L. Asiaticus*. [36] reported *Ca. L. Asiaticus* might prioritize fructose utilization. Thus, *Ca. L. Asiaticus* infection will result in reduced fructose concentrations and glucose accumulation in the infected host tissues. In this study, starch, glucose, and sucrose were accumulated in Las-infected leaves and phloem, whereas fructose did not accumulate in Las-infected phloem. This result was in agreement with observations in previous research. We also analyze the COG function annotation proteins involved in carbohydrate transport and metabolism in the Las-infected plants treated by GJ1 compared with untreated plants. The protein expression of two transferases and four enzymes involved in glycolysis increased. Ribulose-1,5-Bisphosphate Carboxylase/Oxygenase (RuBPCO) take part in the first major carbon fixed reactions in the Calvin cycle during photosynthesis, it catalyzed carbon dioxide converted to energy and storage in biology molecular. The Ribulose-1,5-bisphosphate carboxylase/oxygenase increased 51%. Otherwise, the protein expression of β -galactosidase, α -galactosidase, and pectin lyase also increased in the Las-infected plants treated by GJ1 compared with untreated plants. Notably, the protein expression amount of starch synthase increased by 31.7%, and beta-amylase increased by 1% in the Las-infected plants treated by GJ1 compared with untreated plants. We suggested that starch synthase is normally needed when carbon metabolism trend to balanced. In this study, Beta-amylase 1 (BMY1) (Dt21445) was analyzed by RT-PCR the relative expression was increase 3.9 fold (data not show). 19 Bate-amylase were found in ITRAQ data, although it was not enriched into Differential Abundance Protein (DAP), the beta-amylase probably play a role on in post-translational modification level (methylation, phosphorylation and acetylation), those need investigate further.

B. amyloliquefaciens GJ1 treatment promoted starch degradation

A literature search indicated that starch grains, besides accumulating in every photosynthetic and parenchyma cell of all aerial parts, are also found in phloem sieve elements in Las-infected samples [37, 38]. Phloem blockage is partially due to the deposits of numerous calloses [34]. The PP_2 gene was induced in HLB diseased citrus compared with healthy controls [6]. Starch accumulation has also been reported to increase in infected aerial tissues but depleted in roots. Photosynthesis is repressed, and genes encoding photosystem-II and photosystem-I protein are down regulated by “*Ca. L. Asiaticus*” infection [35]. In our test, four KEGG pathway involved in Photosynthesis were up-regulated in transcriptome in Las-infected plants with GJ1-treated (in press). In this study, the photosynthesis rate increased slightly and needs further investigation under suitable temperatures. We found that the top of roots was not dyed dark blue with theiodine-KI staining in GJ1-treated samples, whereas dark blue and dark red particles were clearly visible in untreated tops of roots. Thus, GJ1 clearly degraded starch. By contrast, leaf sections showed no signs of blue in both GJ1-treated and untreated leaves, the practical change of component and regulatory mechanisms in leaves after GJ1-treatment need further verification.

Conclusion

In this study, a new potential biocontrol agent *B. amyloliquefaciens* GJ1 against HLB was used for the experiment. Differential Abundance Protein (DAP) and COG annotation proteins were elucidated by ITRAQ, particularly proteins relating to carbohydrate transport and metabolism were analyzed. The effect on decreased the accommodation of starch and soluble sugar were proved in Las-infected plants treated by GJ1. The effect of starch degradation was observed in roots of Las-infected plants treated by GJ1. It is significant for us to put forward the new strategy resist Huanglongbing disease.

Author's Contributions

JL presented the ideas and organized the implementation of the project, investigated the condition of I₂-KI reaction, collected and analysis data and compose the manuscript. TJZ, YXY, performed the *Bacillus sp.* GJ1 treatment, analysis and detection of HLB and collected and analysis data. DL, investigated index of health and infected citrus. NJ: performed the earlier sequencing of *Bacillus sp.* GJ1. ZXY: earlier screening of *Bacillus sp.* GJ1. The contribution of TJZ, DYX, DL is equivalent.

Acknowledgement

This research was financially supported by grants from the nation nature science found (No.31572099 and No. 31272146).

References

- Bové JM. Huanglongbing or yellow shoot, a disease of Gondwanan origin: Will it destroy citrus worldwide? *Phytoparasitica*. 2014; 42: 579-583.
- Garnier M, Danel N, Bove JM. The Greening Organism is a Gram Negative Bacterium. In: Garnsey SM, Timmer LW, and Dodds JA(eds.). *Proc 9th Conf Intl Organ Citrus Virologists*. IOCV, Riverside, CA. 1984;115-124.
- Garnier M, Jagoueix-Eveillard S, Cronje PR, Le Roux HF, Bové JM. Genomic characterization of a liberibacter present in an ornamental rutaceous tree, *Calodendrum capense*, in the Western Cape Province of South Africa. Proposal of '*Candidatus Liberibacter africanus* subsp. *capensis*'. *Int J Syst Evol Microbiol*. 2000; 50: 2119-2125.
- Jagoueix S, Bové JM, Garnier M. The phloem-limited bacterium of greening disease of citrus is a member of the alpha subdivision of the proteobacteria. *Int J Syst Bacteriol*. 1994; 44: 379-386.
- Lin KH. Observations on yellow shoot on Citrus. Etiological studies of yellow shoot of Citrus. *Acta Phytopathologica Sinica*. 1956; 2: 1-42.
- Kim JS, Sagaram US, Burns JK, Li J, Wang N. Response of sweet orange (*Citrus sinensis*) to '*Candidatus Liberibacter asiaticus*' infection: microscopy and microarray analyses. *Phytopathology*. 2009; 99: 50-57.
- Aritua V, Achor D, Gmitter FG, Albrigo G, Wang N. Transcriptional and microscopic analyses of citrus stem and root responses to *Candidatus Liberibacter asiaticus* infection. *PLoS One*. 2013; 8: e73742.
- Pourreza A, Lee WS, Etxeberria E, Banerjee A. An evaluation of a vision-based sensor performance in Huanglongbing disease identification. *Biosystems Engineering*. 2015; 130: 13-22.
- da Graça JV, Douhan GW, Halbert SE, Keremane ML, Lee RF, Vidalakis G, et al. Huanglongbing: An overview of a complex pathosystem ravaging the world's citrus. *J Integr Plant Biol*. 2016; 58: 373-387.
- Lopez JA, Durborow SL. Huanglongbing and the California Citrus Industry: A Cost Comparison of Do Nothing vs. Do Something Management Practices. *The Texas Journal of Agriculture and Natural Resources*. 2014; 27: 51-68.
- Rouse RE, Ozores-Hampton M, Roka FM, Roberts P. Rehabilitation of Huanglongbing-affected Citrus Trees Using Severe Pruning and Enhanced Foliar Nutritional Treatments. *HortScience*. 2017; 52: 972-978.
- Hu J, Jiang J, Wang N. Control of Citrus Huanglongbing via Trunk Injection of Plant Activators and Antibiotics. *Phytopathology*. 2018; 108: 186-195.
- Pagliai FA, Gonzalez CF, Lorca GL. Identification of a Ligand Binding Pocket in LdtR from *Liberibacter asiaticus*. *Front Microbiol*. 2015; 6: 1314.
- Doud MM, Wang YS, Hoffman MT, Latza CL, Luo W, Armstrong CM, et al. Solar thermotherapy reduces the titer of *Candidatus Liberibacter asiaticus* and enhances canopy growth by altering gene expression profiles in HLB-affected citrus plants. *Hortic Res*. 2017; 4: 17054.
- Duan Y, Zhou L, Hall DG, Li W, Doddapaneni H, Lin H, et al. Complete genome sequence of citrus huanglongbing bacterium, '*Candidatus Liberibacter asiaticus*' obtained through metagenomics. *Mol Plant Microbe Interact*. 2009; 22: 1011-1020.
- Zou H, Gowda S, Zhou L, Hajeri S, Chen G, Duan Y. The destructive citrus pathogen, '*Candidatus Liberibacter asiaticus*' encodes a functional flagellin characteristic of a pathogen-associated molecular pattern. *PLoS One*. 2012; 7: 464-447.
- Gottwald TR. Current epidemiological understanding of citrus huanglongbing. *Annu Rev Phytopathol*. 2010; 48: 119-139.
- Martinelli F, Reagan RL, Dolan D, Fileccia V, Dandekar AM. Proteomic analysis highlights the role of detoxification pathways in increased tolerance to Huanglongbing disease. *BMC Plant Biol*. 2016; 16: 167.
- Canales E, Coll Y, Hernández I, Portieles R, Rodríguez García M, López Y, et al. '*Candidatus Liberibacter asiaticus*', Causal Agent of Citrus Huanglongbing, Is Reduced by Treatment with Brassinosteroids. *PLoS One*. 2016; 11: e0146223.
- Fu S, Shao J, Zhou C, Hartung JS. Transcriptome analysis of sweet orange trees infected with '*Candidatus Liberibacter asiaticus*' and two strains of Citrus Tristeza Virus. *BMC Genomics*. 2016; 17: 349.
- Rawat N, Kiran SP, Du D, Gmitter FG, Deng Z. Comprehensive meta-analysis, co-expression, and miRNA nested network analysis identifies gene candidates in citrus against Huanglongbing disease. *BMC Plant Biol*. 2015; 15: 184.
- Nwugo CC, Duan YP, Lin H. Study on Citrus Response to Huanglongbing Highlights a Down-Regulation of Defense-Related Proteins in Lemon Plants Upon 'Ca. *Liberibacter asiaticus*' Infection. *PLOS ONE*. 2013; 8: 67442.
- O'Brien PA. Biological control of plant diseases. *Australasian Plant Pathology*. 2017; 46: 293-304.
- Elshaghabee FMF, Rokana N, Gulhane RD, Sharma C, Panwar H. *Bacillus As Potential Probiotics: Status, Concerns, and Future Perspectives*. *Front Microbiol*. 2017; 8: 1490.
- Chowdhury SP, Hartmann A, Gao X, Borriss R. Biocontrol mechanism by root-associated *Bacillus amyloliquefaciens* FZB42 - a review. *Front Microbiol*. 2015; 6: 780.
- Fan B, Carvalhais LC, Becker A, Fedoseyenko D, von Wirén N, Borriss R, et al. *BMC Microbiology*. 2012; 12: 116.
- Harbron S, Foyer C, Walker D. The purification and properties of sucrose-phosphate synthetase from spinach leaves: the involvement of this enzyme and fructose bisphosphatase in the regulation of sucrose biosynthesis. *Arch Biochem Biophys*. 1981; 212: 237-246.
- Sivak MN, Wagner M, Preiss J. Biochemical Evidence for the Role of the Waxy Protein from Pea (*Pisum sativum* L.) as a Granule-Bound Starch Synthase. *Plant Physiology*. 1993; 103: 1355-1359.
- Ritte G, Lloyd JR, Eckermann N, Rottmann A, Kossmann J, Steup M. The starch-related R1 protein is an α-glucan water dikinase. *Proc Natl Acad Science*. 2002; 99: 7166-7171.
- Wang XK. *Principles and Techniques of Plant Physiology and Biochemistry 2nd ed.* Beijing: Higher Education Press. 2006; 124-126.
- Jin YH, Zhang KL, Zhang XC, Du JH. Double wavelength method to determine the content of amylose and amylopectin in wheat and wheat buds. *Journal of Chinese grain and oil*. 2009; 137-140.

32. Robert L, Barry EF. Modern practical gas chromatography. Chemical Industry Press. 2004.
33. Gonzalez P, Reyes-De-Corcuera J, Etxeberria E. Characterization of leaf starch from HLB-affected and unaffected-girdled citrus trees. *Physiological and Molecular Plant Pathology*. 2012; 79: 71-78.
34. Koh EJ, Zhou L, Willians DS, Park J, Ding N, Duan YP, *et al*. Callose deposition in the phloem plasmodesmata and inhibition of phloem transport in citrus leaves infected with '*Candidatus Liberibacter asiaticus*'. *Protoplasma*. 2011; 249: 687-697.
35. Albrecht U, Bowman KD. Gene expression in *Citrus sinensis* (L.) Osbeck following infection with the bacterial pathogen *Candidatus Liberibacter asiaticus* causing Huanglongbing in Florida. *Plant Science*. 2008; 175: 291-306.
36. Fan J, Chen C, Brlansky RH, Gmitter FG, Li ZG. Changes in carbohydrate metabolism in *Citrus sinensis* infected with '*Candidatus Liberibacter asiaticus*'. *Plant Pathology*. 2010; 59: 1037-1043.
37. Etxeberria E, Gonzalez P, Achor D, Albrigo G. Anatomical distribution of abnormally high levels of starch in HLB-affected Valencia orange trees. *Physiological and Molecular Plant Pathology*. 2009; 74: 76-83.
38. Folimonova SY, Achor DS. Early events of citrus greening (Huanglongbing) disease development at the ultrastructural level. *Phytopathology*. 2010; 100: 949-958.